Journal of Atmospheric Chemistry **8** (1989) 139–151.

Spectroscopic Measurements of Atmospheric Carbon Monoxide and Methane. 1: Latitudinal Distribution

V. I. DIANOV-KLOKOV, L. N. YURGANOV*, E. I. GRECHKO, and A. V. DZHOLA
Institute of Atmospheric Physics, Academy of Sciences, Moscow 109017, U.S.S.R.

(Received: 26 August 1987; revised: 3 November 1988)

Abstract. The results of spectroscopic total column measurements of CO and CH_4 at different points of the Northern and Southern Hemispheres in 1970–1985, are reported. Seasonal cycles of CO are evident for all the sites. The Northern Hemispheric long-term positive trend of CO seems to be 1.5–2% per year. In the Southern Hemisphere, temporal increasing was not detected and a possible upper limit for it is about 0.6% per year. Methane concentration in the Northern Hemisphere increases at a rate of 1.2% per year.

Key words. Carbon monoxide, methane, latitudinal distribution, spectroscopic measurements, Arctic, Antarctic.

1. Introduction

Carbon monoxide and methane in the atmosphere are known to be of both natural and anthropogenic origin. The background concentrations of these gases tend to increase as a result of human activity (Dvoryashina *et al.*, 1984; Rasmussen and Khalil, 1981). Both CO and CH_4 are active agents in tropospheric and stratospheric photochemistry with methane oxidation by OH being a significant CO source (Crutzen, 1983). CO and CH_4 are removed from the atmosphere through reactions with OH, thus an increase of background CO and CH_4 concentrations would lead to OH depletion. Moreover, CH_4 and CO are photochemically connected with the tropospheric ozone. CH_4 and O_3 contribute to the greenhouse effect of the atmosphere (Ramanathan *et al.*, 1985). The foregoing clearly indicates the importance of the monitoring of these gases in a clean (unpolluted) atmosphere.

Most of the presently available data have been obtained by the mercury oxide technique (Seiler, 1974) or by gas chromatography (GC) (Rasmussen and Khalil, 1981). These techniques can be used only locally while, for carbon monoxide (a highly variable gas), an extensive spatial averaging is frequently necessary. Such averaging can be achieved by the solar spectroscopic method; at air

---

* Now at the Arctic and Antarctic Research Institute, Leningrad 199226, U.S.S.R.

masses 1.5–2.5, effective atmospheric paths amount to 10–20 km. In the present paper, a spectroscopic method for measuring atmospheric CO and CH_4 is used in a slightly modified form of the method given by Pugachev *et al.* (1978) and Dvoryashina *et al.* (1984). It discusses the results of the geographic distribution of CO and CH_4. The second paper of this issue (Dianov-Klokov and Yurganov, 1989) deals with CO seasonal variations and discusses trends of CO and CH_4 increases during the 1970–80s.

Atmospheric absorption spectra were recorded by spectroscopic equipment (Arefyev *et al.*, 1978) consisting of (1) an automatic solar guiding unit, (2) a large-aperture (1 : 5) monochromator with a grating of 300 lines per mm, with a focal length of 822 mm and a resolution of 0.25–0.30 cm^{-1} in 3.3–4.7 μm, (3) electronics including a PbSe photoconductive cell (cooled by solid carbon dioxide), a lock-in amplifier, and a paper-tape recorder. The equipment operates in fixed location as well as on various mobile platforms (a car or a ship [the latter, under a swell of not more than 4/10]). Figure 1 shows an example of the CO spectrum.

The total column content of a gas U is measured in atm cm STP (layer reduced to STP in cm), 1 atm cm $= 2.69 \times 10^{15}$ mol cm^{-2}. To determine U, the integral absorption within the line contour (equivalent width) W is measured; for CO, we used the $R(3)$ line of the fundamental absorption band and for CH_4, the $P(2)$ line of the ν_3 band (see Figure 1). The straight line connecting the nearest atmospheric windows is assumed as a line of zero absorption. Then using a set of spectral line parameters (AFGL, version of 1982, Rothman *et al.*, 1983), the same spectral region is synthesized and then tuning the gas concentrations, air mass, and air temperature, the optimal relation between U and W can be formulated. The lines of CO and CH_4 are known to overlap those of water vapour (H_2O). Hence, the atmospheric H_2O content is also taken into account in data processing. In the case of CO, it appeared necessary to measure the total water vapour content using a similar technique and the H_2O line centered at 2156.59 cm^{-1} (Figure 1). It should be noted that the values of this line intensity for two versions of AFGL-compilations (Rothman, 1981 and Rothman *et al.*, 1983) differ 1.6 times ($S = 0.107$ and 0.175×10^{-22} cm^{-1}/mol cm^{-2}, respectively). To resolve this problem, the H_2O contents measured spectroscopically during the summers of 1983 and 1984 (surface air temperature >18 °C) were compared with that obtained by Rawinsonde system (Dolgoprudny station, near Moscow). The correct value of S_0 appeared to be between the two above-mentioned values. Therefore, S_0 has been assumed to be 0.14×10^{-22} cm^{-1}/mol cm^{-2} (±15%) and the line half-width $\gamma_0 = 0.07$ cm^{-1}/atm. For the methane case, surface humidity values appeared to be a sufficient indicator of the atmospheric water vapour content. Calculation formulae and tables are given in the Appendix.

The uncertainty of CO abundance due to variations of the gas profile, is quite significant. Numerical experiments were carried out to study this effect. The

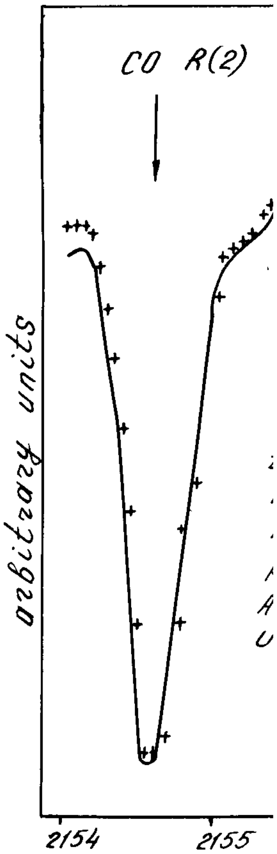

Fig. 1. An example of a
simulated by a computer is

measured CO profil
taken as typical.

Figure 2 indicates
a dramatic decrease
and Lado-Bordowsk
local increase of th
modelled by profile
the dry season (Crut
this case is close to
corresponds to the sa

The six profiles
spectra calculations.
ured' spectra which
mixing ratio $R_m =$

-20 km. In the present
c CO and CH_4 is used
ichev *et al.* (1978) and
geographic distribution
Klokov and Yurganov,
rends of CO and CH_4

ectroscopic equipment
lar guiding unit, (2) a
00 lines per mm, with
) cm^{-1} in 3.3–4.7 μm,
cooled by solid carbon
'he equipment operates
s (a car or a ship [the
ows an example of the

in atm cm STP (layer
$^{-2}$. To determine U, the
width) W is measured;
tion band and for CH_4,
ht line connecting the
absorption. Then using
Rothman *et al.*, 1983),
the gas concentrations,
ween U and W can be
overlap those of water
also taken into account
ary to measure the total
e H_2O line centered at
ies of this line intensity
1 and Rothman *et al.*,
m^{-1}/mol cm^{-2}, respec-
sured spectroscopically
perature >18 °C) were
lgoprudny station, near
tween the two above-
0.14×10^{-22} cm^{-1}/mol
. For the methane case,
ator of the atmospheric
re given in the Appen-

the gas profile, is quite
study this effect. The

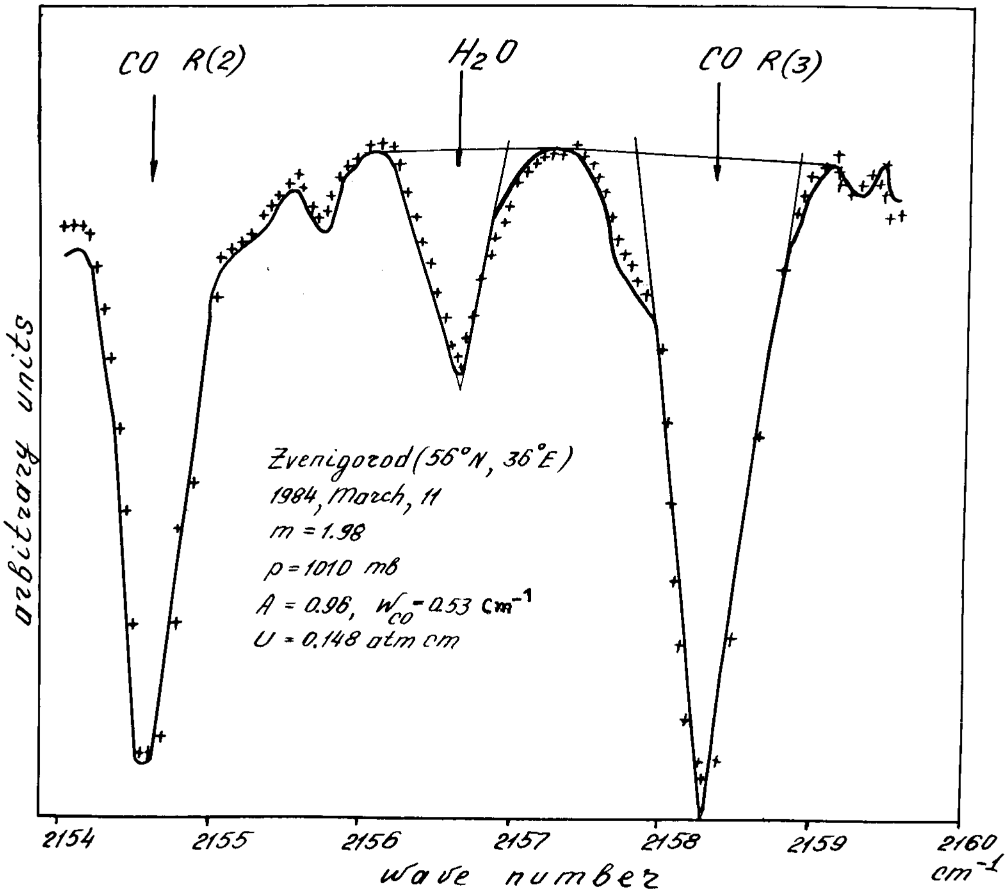

Fig. 1. An example of a spectrogram for the fundamental CO band (solid line). The spectrum simulated by a computer is shown by crosses.

measured CO profiles (Seiler and Fishman, 1981; Crutzen *et al.*, 1985) were taken as typical.

Figure 2 indicates the CO mixing ratio which decreases with height, with a dramatic decrease to 50 ppbv at the tropopause (200–250 mb) (Louisnard and Lado-Bordowsky, 1983). For some real profiles (Nos. 2, 3, 4), there is a local increase of the mixing ratio value in the upper troposphere which is modelled by profile No. 5. Profile No. 1 is typical of Brasilian savannah fires in the dry season (Crutzen *et al.*, 1985). Apparently, in a natural environment, this case is close to an extreme situation. Modelled step-like profile No. 6 corresponds to the same total CO content as the real profile No. 1.

The six profiles of Figure 2 have been used as initial data for computer spectra calculations. Calculated in this way, spectra are assumed to be 'measured' spectra which yield the so-called 'measured' values of U_m and the mean mixing ratio $R_m = U_m/H_0$ ($H_0 = 7.9$ km, the atmospheric scale height) as is

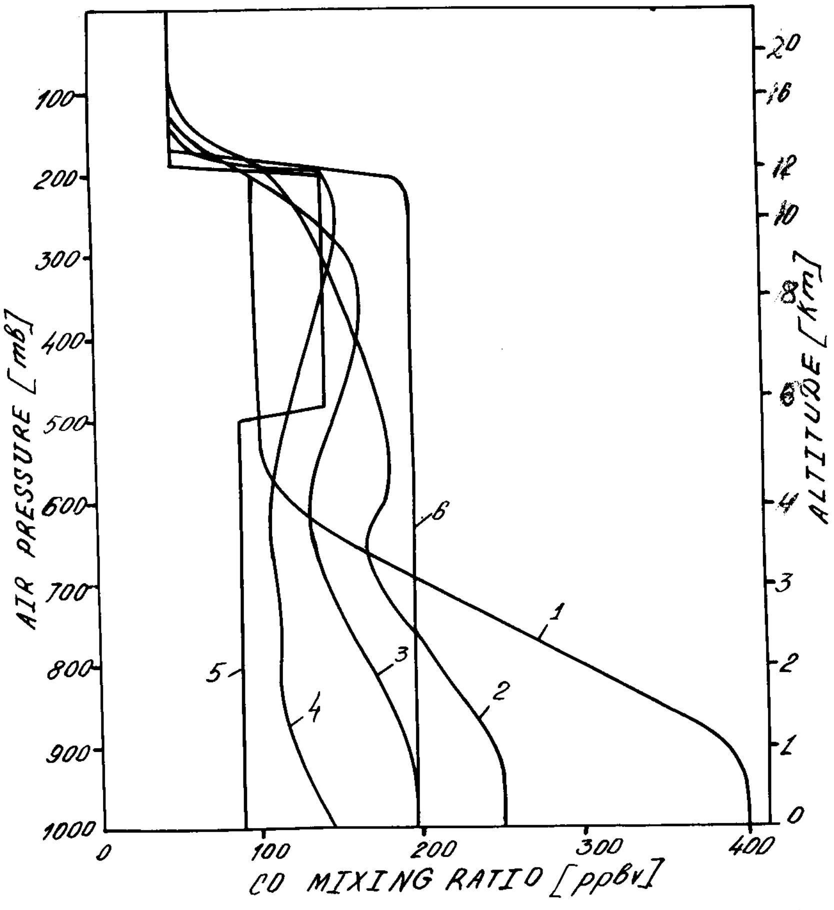

Fig. 2. Vertical CO profiles used as initial data for a numerical experiment studying the errors of measurements due to profile uncertainty. (1) mean profile for burning savannah (Crutzen *et al.*, 1985); (2), (3), (4), directly measured midlatitude profiles (Seiler and Fishman, 1981); (5) and (6), simulated profiles.

usually done for real measured spectra (Table I, columns 5 and 6). The second column of Table I presents the so-called 'true' (those used in the computer simulations) values of the total contents U_t, while columns 3 and 4 present mean 'true' mixing ratios for the whole of the atmosphere and troposphere, respectively. Column 7 indicates the 'measured' total contents to be higher than the 'true' values for all the cases. For 'Savannah fires' (extraordinary profile No. 1) the excess is 23%. Thus, the CO total content uncertainty is significant (see Table I) and strongly dependent on CO vertical distribution. On the other hand, the difference between the measured mean tropospheric CO mixing ratio and the real one is within ≈5%. It seems to be caused by measuring atmospheric mean weighted mixing ratios rather than simple atmospheric averages, while the contribution of the tropospheric layers is predominant. This fact becomes

Table I. Results of a nun
content versus height distribut

Prof.	'True'	
No.	U_t	$R_t =$
(1)	(2)	(3)
1	0.130	164
2	0.123	156
3	0.107	136
4	0.085	108
5	0.077	97
6	0.130	164

Values of U are given in the a

clear if we take into a
is significantly greater t
(because the tropospher
in the troposphere obsc

All results presente
Yurganov, 1989), have
versus altitude. At a fir
tions show that it leads
But obtained in this w
mean tropospheric C
informative than the to

For midlatitudes (p
tions of CO profile, car
of a single measureme
random rms uncertain
(e.g. a month), decrease

2. Results

Carbon monoxide and
The latitudinal distrit
content between the N
(Seiler, 1974; Malkov
et al., 1982).

The inhomogeneity
variations, results in a
its latitudinal distribut

This paper presen

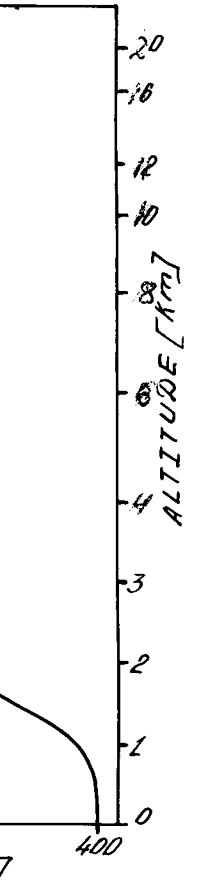

ient studying the errors of
savannah (Crutzen *et al.*,
shman, 1981); (5) and (6),

5 and 6). The second
sed in the computer
nns 3 and 4 present
ere and troposphere,
nts to be higher than
extraordinary profile
ertainty is significant
bution. On the other
eric CO mixing ratio
easuring atmospheric
ieric averages, while
t. This fact becomes

Table I. Results of a numerical experiment, studying the dependence of measured gas content versus height distribution

Prof.	'True'			'Measured'			R_m
No.	U_t	$R_t = \frac{U_t}{H_0}$	R_t(trop)	U_m	$R_m = \frac{U_m}{H_0}$	$\frac{U_m}{U_t}$	R_t(trop)
(1)	(2)	(3)	(4)	(5)	(6)	(7)	(8)
1	0.130	164	197	0.160	203	1.23	1.03
2	0.123	156	186	0.141	179	1.15	0.96
3	0.107	136	160	0.120	152	1.12	0.95
4	0.085	108	124	0.092	116	1.08	0.94
5	0.077	97	110	0.079	100	1.02	0.91
6	0.130	164	197	0.144	183	1.11	0.93

Values of U are given in the atm cm; R, in ppbv. For profile numbers, see caption for Figure 2.

clear if we take into account that the spectral line width in the troposphere is significantly greater than that in the stratosphere. Thus, the wide and strong (because the troposphere constitutes about 80% of the atmosphere) lines formed in the troposphere obscure the narrow and weak stratospheric lines.

All results presented in this and the following paper (Dianov-Klokov and Yurganov, 1989), have been obtained by assuming a constant CO mixing ratio versus altitude. At a first glance, it is an unrealistic suggestion, and the calculations show that it leads to 8–15% over the estimation of the total CO contents. But obtained in this way, the CO mixing ratio R_m is a good estimation of the mean tropospheric CO mixing ratio. For many applications, R_m is more informative than the total content.

For midlatitudes (profiles Nos. 2, 3, 4), random errors of R_T, due to variations of CO profile, can be estimated as ±4%. The total random rms uncertainty of a single measurement appears to be ±(8–10)% (see the Appendix). The total random rms uncertainty of the average over a set of spectra for a long period (e.g. a month), decreases down to ±(4–5)%.

2. Results

Carbon monoxide and methane seem to have different latitudinal distributions. The latitudinal distribution of CO demonstrates a pronounced difference in content between the Northern Hemisphere (NH) and Southern Hemisphere (SH) (Seiler, 1974; Malkov *et al.*, 1976), while that of CH_4 is less (about 6%) (Mayer *et al.*, 1982).

The inhomogeneity of CO spatial distribution accompanied by its seasonal variations, results in a considerable variation of this gas. To make the pattern of its latitudinal distribution, one should obtain a set of latitudinal sections.

This paper presents the results of spectroscopic measurements obtained

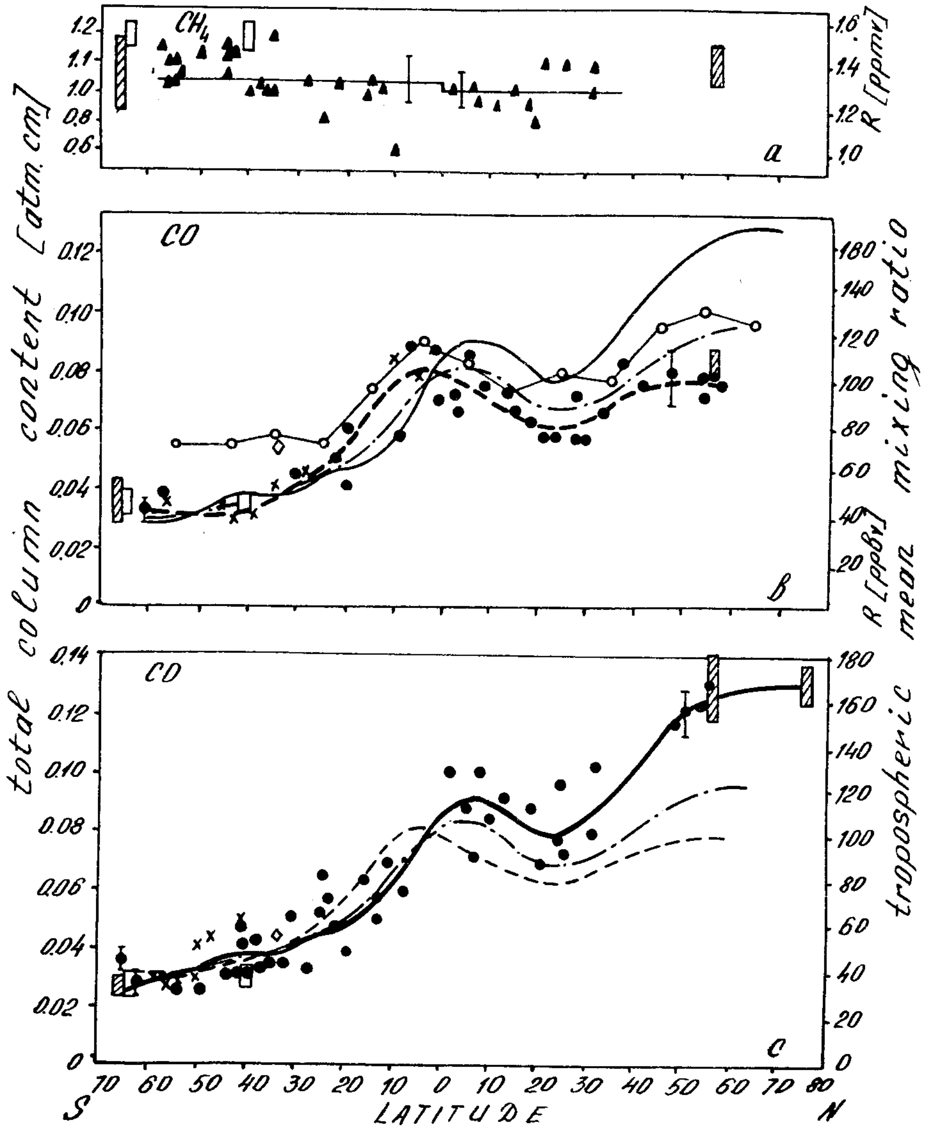

Fig. 3. Latitudinal distributions of CH_4 (triangles, top panel) and CO (middle and bottom panels); the middle panel is for May, June, November, December (first period) and the bottom one is for the period from January to April (second period).

Full circles show values of CO content averaged over 5–20 spectra for the Atlantic sector; crosses indicate the same values for the Pacific sector. Smooth lines are spline approximations: dashed line, for the first period, solid line, for the second period, dash and dotted line, for the whole set of data. Open circles, linked by a broken line, demonstrate the mean values of the mixing ratio in the free troposphere of the Atlantic sector (Seiler and Fishman, 1981). Shaded rectangles depict the data of our observations; empty rectangles, the data by Fraser *et al.* (1986 see text); diamonds, for the South Africa (Seiler *et al.*, 1984). Horizontal lines are the mean contents of CH_4 for both hemispheres.

during four sea exped
et al., 1976; Yurgan
Grechko, 1986) using
In order to take into a
two groups: the first g
period adjoining the C
second group (Figure
maximum, according
data for the Atlantic (
are represented, respe
tudinal distributions p
parts of the world and
data was obtained du
background concentra
(Dvoryashina *et al.*, 19
smoothed by cubic sp
line for the second gr
comparison, three spli
sea expeditions are sh
rectangles) measured a
(Voskresensky *et al.*,
Arctic station on Zhok

Figure 3 demonstra
north to the south. Me
the year. Solid and dah
latitudinal distribution
near the Equator, and
minimum at 25° N. T
measurements conduct
July–August 1974 (op
data set does not differ
25° S (not more than
methods applied). It a
continues to decrease c
Seiler and Fishman (1
results (70 ppbv) have
surface layer in South
that our data set for the
of the SH, namely near
for the same month at
(Eraser *et al.*, 1986). A
of other groups seem to
measurements. The rea

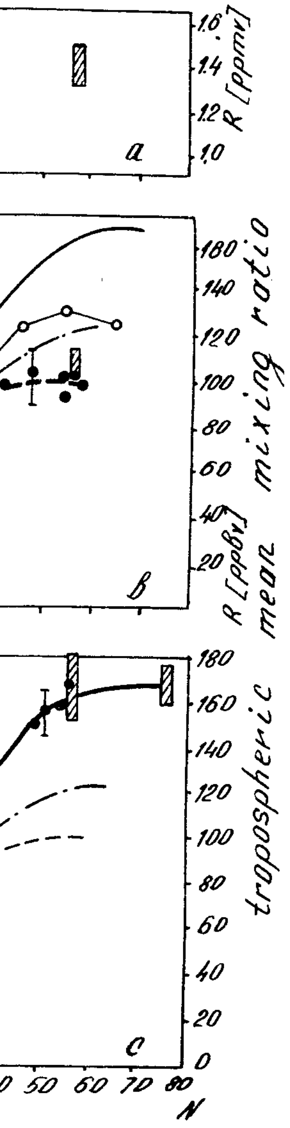

niddle and bottom panels);
and the bottom one is for

ra for the Atlantic sector;
are spline approximations:
h and dotted line, for the
e the mean values of the
l Fishman, 1981). Shaded
ata by Fraser *et al.* (1986
ines are the mean contents

during four sea expeditions in different oceans and seasons of the year (Malkov *et al.*, 1976; Yurganov *et al.*, 1979; Dianov-Klokov and Yurganov, 1982; Grechko, 1986) using the same spectroscopic parameters (Rothman *et al.*, 1983). In order to take into account the seasonal variations, the data were divided into two groups: the first group (Figure 3b) – May, June, November, December (the period adjoining the CO seasonal minimum in the Northern Hemisphere); the second group (Figure 3c) – from January to April (the period, adjoining the maximum, according to Dianov-Klokov and Yurganov, 1981). Moreover, the data for the Atlantic (westward of 70° E) and Pacific (eastward of 110° E) areas are represented, respectively, by dots and crosses (Fig. 3b, c). Hence, the latitudinal distributions presented here, appear to be typical of the corresponding parts of the world and periods of the year. It should be noted that the bulk of the data was obtained during the period of 1978–1983. During that period, CO background concentration was believed to increase by 10% as a maximum (Dvoryashina *et al.*, 1984; Dianov-Klokov and Yurganov, 1989). The data were smoothed by cubic splines; a dashed line, for the first group of results, a solid line for the second group, and a dash-and-dot line for the whole data set. For comparison, three splines are plotted twice (Figures 3b, 3c). The results of the sea expeditions are shown together with the ranges of CO variations (shaded rectangles) measured at the Antarctic stations Molodezhnaya and Mirny (68° S), (Voskresensky *et al.*, 1986), in Zvenigorod (near Moscow, 56° N), and at the Arctic station on Zhokhov Island (76° N, 153° E) (Gabrielyan *et al.*, 1984).

Figure 3 demonstrates a pronounced decrease of the atmospheric CO from north to the south. Meanwhile, the slope of the curve depends on the season of the year. Solid and dahsed curves bound the range of temporal variations of the latitudinal distribution. All three curves are characterized by two maxima: one near the Equator, and the other in the northern midlatitudes, and by the local minimum at 25° N. The same distribution is evident in the data of aircraft measurements conducted over Europe and northern and southern America in July–August 1974 (open circles, Figure 3b, (Seiler and Fishman, 1981)). The data set does not differ greatly from that of ours for the territory from 65° N to 25° S (not more than 10–20%, which can be explained by the difference in methods applied). It appears from our data that the CO mean mixing ratio continues to decrease down to 40 ppbv southward of 25° S, while, according to Seiler and Fishman (1981), it becomes stable at the 70 ppbv level. The same results (70 ppbv) have been obtained by Seiler *et al.* (1984) for the atmospheric surface layer in South Africa (34° S) (Figure 3b, diamond). It should be noted that our data set for the region southward of 25° S was obtained in the other part of the SH, namely near Australia. Figure 3b also gives GC data (open rectangles) for the same month at Tasmania (41° S, 145° E) and at Mawson (68° S, 63° E) (Eraser *et al.*, 1986). Apparent differences between Seiler's data and the results of other groups seem to be larger than natural fluctuations and uncertainties of measurements. The reason for this disagreement is still not evident.

Figure 3a also presents latitudinal distributions of CH_4 (triangles). The values were averaged separately for the SH and the NH. The results are given as follows: NH; $U = 1.03 \pm 0.06$ atm cm (11 days of measurements); SH; $U = 1.06 \pm 0.08$ atm cm (23 days of measurements). The scatter of the data points approximates the uncertainty of the measurements (±8%). Within these scatter ranges, apparent differences in the CH_4 content have not been detected between the two hemispheres. The Arctic abundance of CH_4 does not demonstrate any peculiar feature (Gabrielyan *et al.*, 1984) (Figure 3a, dashed rectangle).

3. Conclusions

The spectroscopic technique used in this study has a few special features compared to local methods (e.g. GC). The measurements result in a weighted mean mixing ratio for the whole atmosphere which differs from the tropospheric simple average by 6% as a maximum. Such spatial averaging allows a smoothing of the random fluctuations of gas concentrations (including anthropogenic ones).

The second feature is manifested in the procedure of calibration. Local methods require the calibration of every measurement using calibration mixtures. In the case of the spectroscopic technique, the calibration procedure is transferred to the step of obtaining spectral line parameters. Due to this feature, the results of different measurements are comparable if the scientists use the same set of spectral line parameters. Moreover, it is easier to compare the data of different years of observation.

The spectroscopic technique aids in obtaining the latitudinal distribution of CO (carbon monoxide) in the area between 80° N and 70° S. The seasnal variability of the latitudinal CO profiles has been distinguished by this technique. As was mentioned before (Dianov-Klokov and Yurganov, 1981), the slope of the CO distribution is steeper in the period from January to April, than in the period May, June, November and December. The distributions have a two-humped pattern with the maxima in the midlatitudes of the NH (obviously, anthropogenic maximum) and in the tropics (its possible causes are forest and savannah fires, photochemical processes, etc. (see Crutzen *et al.*, 1985)). Attention is drawn to the latitudinal zone between 30° S and 60° S, which is possibly characterized by a pronounced difference in the CO mixing ratio between the Pacific and Atlantic regions, particularly in winter (SH).

Methane measurements do not reveal hemispheric differences in its content, larger than the uncertainties of measurements (see also, Grechko, 1986).

Appendix

Algorithm of Spectrum P

(a) CO:

(1) Plot the condition
parent windows 21

(2) Draw the lateral
contour of the CO

(3) Do the same oper
the wavelengths of

(4) Determine the 'eq

$$W = \frac{S}{y} \cdot \frac{\Delta \nu}{\Delta X},$$

where S is the ar
line, and ΔX and
and the referent H

(5) Determine the tot
atmospheric colum

$$w = \frac{W^2(H_2O)}{m \cdot 0.051}$$

$$w = \frac{W^2(H_2O)}{m \cdot 0.035} \cdot$$

where p is the air
the air mass.

(6) Estimate the CO
reduced to sea leve

$$U = \frac{W^2(CO)}{mA} \cdot$$

where

$A = 0.96$ at $w <$

and

$A = 0.83 + 0.10$

(b) CH_4

The procedure of spectr
are as follows.

(1) The positions of th

(triangles). The values
results are given as
measurements); SH;
e scatter of the data
($\pm$8%). Within these
ave not been detected
e of CH_4 does not
4) (Figure 3a, dashed

special features com-
lt in a weighted mean
rom the tropospheric
ng allows a smoothing
anthropogenic ones).
of calibration. Local
nt using calibration
libration procedure is
s. Due to this feature,
the scientists use the
r to compare the data

tudinal distribution of
° S. The seasnal varia-
by this technique. As
981), the slope of the
to April, than in the
ibutions have a two-
f the NH (obviously,
causes are forest and
et al., 1985)). Atten-
0° S, which is possibly
ing ratio between the

erences in its content,
echko, 1986).

Appendix

Algorithm of Spectrum Processing

(a) CO:

(1) Plot the conditional 'line of zero absorption' (base line) through transparent windows 2157.20 and 2159.05 cm^{-1} (Figure 1).

(2) Draw the lateral sides of the triangle, approximating the instrumental contour of the CO line $R(3)$.

(3) Do the same operations with the line H_2O, centered near 2156.59 cm^{-1}; the wavelengths of the windows are 2156.05 and 2157.20 cm^{-1}.

(4) Determine the 'equivalent widths' of both lines by the formula

$$W = \frac{S}{y} \cdot \frac{\Delta \nu}{\Delta X}, \tag{1}$$

where S is the area of the triangle (mm^2), y is the height of the base line, and ΔX and $\Delta \nu = 1.71$ cm^{-1} are the distances between the CO line and the referent H_2O line in mm and cm^{-1}, respectively.

(5) Determine the total content of the water vapour w (g/cm^2) in the vertical atmospheric column reduced to sea level and an air pressure of 1013 mb

$$w = \frac{W^2(H_2O)}{m \cdot 0.051} \left(\frac{1013}{p}\right)^{3.8} \cdot \left(\text{at } \frac{W^2}{m} < 0.14 \text{ cm}^{-2}\right), \tag{2}$$

$$w = \frac{W^2(H_2O)}{m \cdot 0.035} \cdot \left(\frac{1013}{p}\right)^{3.8} - 1.14 \left(\text{at } \frac{W^2}{m} \geqslant 0.14 \text{ cm}^{-2}\right), \tag{3}$$

where p is the air pressure at the level of the instrument in mb and m is the air mass.

(6) Estimate the CO abundance U in atm cm STP ($T = 273$ K, $p = 1$ atm), reduced to sea level and surface air pressure 1013 mb

$$U = \frac{W^2(CO)}{mA} \cdot \left(\frac{1013}{p}\right)^{1.5} \tag{4}$$

where

$$A = 0.96 \text{ at } w < 1.2 \text{ g/cm}^2 \tag{5}$$

and

$$A = 0.83 + 0.108w \text{ at } w \geqslant 1.2 \text{ g/cm}^2. \tag{6}$$

(b) CH_4

The procedure of spectrum processing is practically the same. The differences are as follows.

(1) The positions of the windows are 2997.5 and 3000.2 cm^{-2}.

Table II. Values of A for CH_4 in (4) versus surface air temperature (t °C) and relative humidity r(%)

r% \ t°	-30	-25	-20	-15	-10	-5	0	+5	+10	+15	+20	+25	+30	+35
10	0.295	0.286	0.277	0.269	0.261	0.252	0.245	0.239	0.233	0.227	0.233	0.221	0.229	0.231
30								0.240	0.236	0.235	0.236	0.240	0.258	0.268
40								0.241	0.238	0.237	0.239	0.247	0.270	0.285
50	0.295	0.286	0.277	0.269	0.261	0.253	0.247	0.242	0.239	0.239	0.244	0.254	0.280	0.308
60								0.244	0.241	0.243	0.250	0.263	0.292	0.325
70							0.248	0.245	0.246	0.247	0.254	0.271	0.309	0.362
90								0.246	0.248	0.253	0.267	0.288	0.339	0.380
100	0.295	0.286	0.277	0.269	0.261	0.254	0.250	0.247	0.252	0.256	0.271	0.301	0.350	0.405

Table III. Initial data in calcul

Central frequency of the analytical spectral line cm^{-1}, it identification

Computed spectral range, cm^{-}

Number of absorption lines

Width of slit function, cm^{-1}

Intensity (cm^{-1} mol^{-1} cm^{-2}) and half-width (cm^{-1} atm^{-1}) of the analytical line

Coefficient n for temperature dependence of γ

$$\gamma = \gamma_0 \left(\frac{T}{T_0} \right)^n$$

Fraunhofer lines

[a] $0.329(-18) = 0.329 \times 10^{-18}$.

(2) The wavenumb $\nu_0 = 3001.09$ cm

(3) The relative hu total content. T data for spectra

Random Uncertainties

(1) The uncertainty in

(2) The uncertainty o tional to the gas to spectrum. Hen day. The root-me area estimations, fluctuations, noise amounts to ±(4–6

(3) The daily value o estimation are cau

Table III. Initial data in calculations of model spectra

	CO	CH_4
Central frequency of the analytical spectral line cm^{-1}, its identification	2158,30; $R(3)$ ν_1	(I) 2998.99 $P(2)$, (II) 2999.06
Computed spectral range, cm^{-1}	2152–2160	2994.5–3003.5
Number of absorption lines	18(CO), 36(H_2O), 77(N_2O)	227(CH_4), 56(H_2O) 66(O_3)
Width of slit function, cm^{-1}	0.24	0.30
Intensity (cm^{-1} mol^{-1} cm^{-2}) and half-width (cm^{-1} atm^{-1}) of the analytical line	$S_0 = 0.329(-18)$[a] $\gamma_0 = 0.077$	0.464(–19) (I) 0.155(–19) (II) 0.065 (I) 0.053 (II)
Coefficient n for temperature dependence of γ	$n = 0.5$	$n = 0.5$
$\gamma = \gamma_0 \left(\frac{T}{T_0} \right)^n$		
Fraunhofer lines	included	not included

[a] $0.329(-18) = 0.329 \times 10^{-18}$. I and II – the components of $P(2)$ – doublet.

(2) The wavenumber of the CH_4 line centre $\nu_0 = 2998.91$ cm^{-1}; the line $\nu_0 = 3001.09$ cm^{-1} is used as a reference ($\Delta\nu = 2.18$ cm^{-1}).

(3) The relative humidity of the surface is used as an indicator of the H_2O total content. The values of A in (4) are listed in Table II and the initial data for spectra simulation are presented in Table III.

Random Uncertainties

(1) The uncertainty in computing air mass m is small.

(2) The uncertainty of W measurement. In practice W^2/m, a value proportional to the gas content, demonstrates random variations from spectrum to spectrum. Hence, hourly averages appear to be constant during one day. The root-mean-square deviations of W^2/m include errors of line-area estimations, uncertainties due to transparency variations, air pressure fluctuations, noises of amplifier, fluctuations of gas content, humidity, and amounts to ±(4–6)%.

(3) The daily value of A is assumed to be constant. Some uncertainties of 'A' estimation are caused by

3.1. Variations of A with different m: ±2%.
3.2. Variation of A with different content of the gas U: ±3%.
3.3. Uncertainties due to the error of estimation of the H_2O content: ±2%.
3.4. Due to variations of temperature profiles: ±2%.
3.5. Due to variations of the shape of the CO profile during the day o measurements: ±4%.

Provided that the uncertainties are statistically independent, the rms uncertainty of the gas content is ±8–10%.

Acknowledgements

The authors express their appreciation to Dr N. Pugachev for his help in developing the computer methods of spectra simulation. Thanks are also given to Dr I. Malkov and A. Voskresensky, who organized and carried out some of th measurements.

References

Arefyev, V. N., Dianov-Klokov, V. I., and Malkov, I. P., 1978, Field spectral apparatus for studyin atmospheric pollutants, *Trudy IEM* **8**(81), 73–78 (in Russian).

Crutzen, P. J., 1983, Atmospheric interactions – homogeneous gas reactions of C, N and S containing compounds, in B. Bolin and R. B. Cook (eds.), *The Major Biogeochemical Cycles an their Interactions, SCOPE*, pp. 67–113.

Crutzen, P. J., Delany, A. C., Greenberg, J., Haagenson, P., Heidt, L., Lueb, R., Pollock, W., Seiler, W., Wartburg, A., and Zimmerman, P., 1985, Tropospheric chemical composition measurements in Brasil during dry season, *J. Atmos. Chem.* **2**, 233–256.

Dianov-Klokov, V. I. and Yurganov, L. N., 1981, A spectroscopic study of the global space-tim distribution of atmospheric CO, *Tellus* **33**, 262–273.

Dianov-Klokov, V. I. and Yurganov, L. N., 1989, Spectroscopic measurements of atmospheric carbo monoxide and methane. 2: Seasonal variations and long-term trends, *J. Atmos. Chem.* **8**, 153–16 (this issue).

Dianov-Klokov, V. I. and Yurganov, L. N., 1989, Spectroscpic measurements of the atmospheri carbon monoxide and methane. 2: Seasonal variations and long-term trends, *J. Atmos. Chem* **8**, 000–000 (this issue).

Dvoryashina, E. V., Dianov-Klokov, V. I., and Yurganov, L. N., 1984, On the carbon monoxid atmospheric abundance variations for 1970–1982, *Izv. Akad. Nauk. SSSR, Ser. Fiz. atmosfer.* *Okeana* **20**, 40–47 (in Russian).

Fraser, P. J., Hyson, P., Rasmussen, R. A., Crawford, A. J., and Khalil, M. A. K., 1986, Methane, carbon monoxide and methylchloroform in the Southern Hemisphere, *J. Atmos. Chem.* **4**, 3–42.

Gabriyelyan, A. G., Grechko, E. I., and Dianov-Klokov, V. I., 1983, Spectroscopic measurements o the CO, CH_4 and N_2O total contents in the atmosphere of the Arctic region, *Izv. Akad. Nauk SSSR, Ser. Fiz. atmosfer. i Okeana* **19**, 427–430 (in Russian).

Gabriyelyan, A. G., Grechko, E. I., Dzhola, A. V., Dianov-Klokov, V. I., and Yurganov, L. N., 1984, On the space distribution of carbon monoxide background in the atmosphere at th Northern and Southern Hemispheres, *Izv. Akad. Nauk. SSSR, Ser. Fiz. atmosfer. i Okeana* **20**, 1131–1135 (in Russian).

Grechko, E. I., 1987, Investigation of latitude distribution of the contents of minor atmospheri constituents over ocean, *Izv. Akad. Nauk. SSSR, Ser. Fiz. atmosfer. i Okeana* **23**, 99–102 (i Russian).

Lousnard, N. and Lado-Bo the atmosphere, *J. Geop*

Mayer, E. W., Blake, D. R. Methane: interchemisp *Natl. Acad. Sci. U.S.A.*

Pugachev, N. S., Tarabukhi amount of atmospheric **14**, 1283–1289 (in Russi

Rasmussen, R. A. and Kh cycles, *J. Geophys. Res.*

Ramanathan, V., Cicerone potential role in climate

Rothman, L. R., 1981, AF *Appl. Opt.* **20**, 791–795.

Rothman, L. R., Gamache Flaud, J.-M., and Ca compilation: 1982 editi

Seiler, W., 1974, The cycle

Seiler, W. and Fishman, troposphere, *J. Geophys*

Seiler, W., Giehl, H., Bru in the Southern Hemisp

Shaw, J. H., 1958, The *Astrophys. J.* **128**, 428–

e gas U: ±3%.

n of the H_2O content: ±2%.

±2%.

O profile during the day of

ly independent, the rms un-

ugachev for his help in devel-
. Thanks are also given to Drs
and carried out some of the

Field spectral apparatus for studying
n).
us gas reactions of C, N and S con-
he Major Biogeochemical Cycles and

, Heidt, L., Lueb, R., Pollock, W.,
Tropospheric chemical composition:
2, 233–256.
copic study of the global space-time

c measurements of atmospheric carbon
n trends, *J. Atmos. Chem.* **8**, 153–164

ic measurements of the atmospheric
d long-term trends, *J. Atmos. Chem.*

N., 1984, On the carbon monoxide
ad. Nauk. SSSR, Ser. Fiz. atmosfer. i

nd Khalil, M. A. K., 1986, Methane,
emisphere, *J. Atmos. Chem.* **4**, 3–42.
1983, Spectroscopic measurements of
f the Arctic region, *Izv. Akad. Nauk.*
n).
Klokov, V. I., and Yurganov, L. N.,
ackground in the atmosphere at the
SSR, Ser. Fiz. atmosfer. i Okeana **20**,

f the contents of minor atmospheric
z. atmosfer. i Okeana **23**, 99–102 (in

Lousnard, N. and Lado-Bordowsky, O., 1983, Spectroscopic measurements of carbon monoxide in the atmosphere, *J. Geophys. Res.* **88**, 3789–3797.

Mayer, E. W., Blake, D. R., Tyler, S. C., Makide, G., Montague, D. C., and Rowland, F. S., 1982, Methane: interchemispheric concentration gradient and atmospheric residence time, *Proc. Natl. Acad. Sci. U.S.A.* **79**, 1366–1370.

Pugachev, N. S., Tarabukhin, V. M., and Yurganov, L. N., 1978, On the methods of measuring total amount of atmospheric carbon monoxide, *Izv. Akad. Nauk. SSSR, Ser. Fiz. atmosfer. i Okeana* **14**, 1283–1289 (in Russian).

Rasmussen, R. A. and Khalil, M. A. K., 1981, Atmospheric methane (CH_4): trends and seasonal cycles, *J. Geophys. Res.* **86**, 9826–9832.

Ramanathan, V., Cicerone, R. J., Singh, H. B., and Kiehl, J. T., 1985, Trace gas trends and their potential role in climate change, *J. Geophys. Res.* **90**, 5547–5566.

Rothman, L. R., 1981, AFGL atmospheric absorption line parameters compilation: 1980 version, *Appl. Opt.* **20**, 791–795.

Rothman, L. R., Gamache, R. R., Barbe, A., Goldman, A., Gillis, J. K., Brown, L. R., Toth, R. A., Flaud, J.-M., and Camy-Peyret, C., 1983, AFGL atmospheric absorption line parameters compilation: 1982 edition, *Appl. Opt.* **22**, 2247–2256.

Seiler, W., 1974, The cycle of atmospheric CO, *Tellus* **26**, 116–135.

Seiler, W. and Fishman, J., 1981, The distribution of carbon monoxide and ozone in the free troposphere, *J. Geophys. Res.* **86**, 7255–7265.

Seiler, W., Giehl, H., Brunke, E.-J., and Halliday, E., 1984, The seasonality of CO abundance in the Southern Hemisphere, *Tellus* **36B**, 219–231.

Shaw, J. H., 1958, The abundance of atmospheric carbon monoxide above Columbus, Ohio, *Astrophys. J.* **128**, 428–440.